Locking behavior of three coupled laser oscillators

H. Erzgräber and S. Wieczorek
School of Engineering, Computing and Mathematics, University of Exeter, Exeter EX4 4QF, United Kingdom

B. Krauskopf
Department of Engineering Mathematics, University of Bristol, Bristol BS8 1TR, United Kingdom

(Received 23 March 2009; published 20 August 2009)

Single-frequency operation or locking in a lateral array of three laser oscillators is studied within the composite-cavity-mode approach. We compute the regions of stable locking, which have a nontrivial shape in the plane of coupling strength versus frequency detuning. The locking regions depend drastically on the amount of amplitude-phase coupling of the lasing field that is quantified by the α parameter. For small α, locking is possible for arbitrary coupling, but only if the middle laser has sufficient frequency detuning from the two outer lasers. In contrast, for larger α, locking is only possible for weak to moderate coupling, provided that all three lasers have similar frequencies.

DOI: 10.1103/PhysRevE.80.026212 PACS number(s): 05.45.Gg, 02.30.Ks, 02.30.Oz

I. INTRODUCTION

Compact sources of high-power coherent radiation are strongly desired in fundamental science (e.g., for spectroscopy) and various applications, including material processing (e.g., cutting, welding), medicine (e.g., laser surgery), and entertainment (e.g., large-scale laser displays). The commonly used broad-area semiconductor lasers suffer from difficult to control spatiotemporal instabilities and poor beam quality at high optical powers [1–3]. As technological progress makes it feasible to produce more sophisticated laser devices, lateral laser arrays emerged as an interesting alternative for generating optical beams that combine high power and quality [4–16]. While they are more promising than broad-area lasers, laser arrays too exhibit various instabilities and complex dynamical behavior. Often, additional optical elements, such as an external mirror or a synchronizing master laser, are used in an attempt to stabilize laser arrays [4,12,15,16], leading to involved optical designs. There has been important previous work on stability of single-frequency operation or locking in a coupled laser device *on its own* [4,7,17–19], but some basic questions still remain unexplored. In particular, a better understanding of coupled laser stability in dependence on key array parameters, such as different widths of individual lasers, would be very desirable. In this respect, three laterally coupled lasers form the simplest system with an underlying structure that is also found in larger arrays. Hence, the study of the three-laser array constitutes a first step toward understanding the stability properties of large arrays.

In this paper we show that a linear array of three nearest-neighbor coupled laser oscillators exhibits interesting locking behavior that is fundamentally different from two-oscillator systems [20]. Specifically, we consider a spatiotemporal composite-cavity model as in [17], where a similar three-laser geometry has been used to evaluate the influence of spatial gain variation. Here, we present a bifurcation analysis of such a model to unveil the complicated dependence of stable locking on the relevant system parameters. First of all, we determine the dependence of stable locking on the coupling strength and on the detuning of the middle laser from two identical outer lasers. One key finding is the strong dependence of the type and extent of stable locking on the amount of amplitude-phase coupling in the lasing field [21]. In lasers the amplitude-phase coupling is quantified by the well-known α parameter, also called the linewidth-enhancement factor [22]. It has typical values of $\alpha \approx 0$ (e.g., for gas, crystal, and quantum dot semiconductor lasers) and $1 < \alpha < 10$ (e.g., for widely used bulk and quantum-well semiconductor lasers) [23]. Second, we study modifications to the locking region arising from different frequencies of outer lasers and different distances between neighboring lasers. Hence, our results contribute to the better understanding of amplitude-phase coupling effects on synchronization in coupled (laser) oscillators, which are also of technological importance for the design of locked laser arrays.

This article is structured as follows. In Sec. II we describe the laser system and the modeling approach. Sec. III discusses the influence of the linewidth-enhancement factor for the symmetrical case where the two outer laser are identical. In Sec. IV we consider effects of breaking this symmetry. We finish with conclusions in Sec. V.

II. COMPOSITE CAVITY MODEL

We consider a laser device consisting of three laser stripes $\{A,B,C\}$ oriented along the longitudinal z direction in which the laser beam is propagating, and coupled in the lateral x direction. To analyze spatiotemporal instabilities in the laser array we decompose the total electric field in terms of spatial composite-cavity mode profiles $X_j(x)$ of the entire array [24,25],

$$\mathcal{E}(x,t) = \frac{1}{2}\sum_j E_j(t)X_j(x) + \text{c.c.}, \tag{1}$$

where the $E_j(t)$ are the complex-valued time-dependent field amplitudes. Following Refs. [17,26] we focus on the x direction only. Hence, the composite-cavity mode profiles $X_j(x)$ are solutions of the Helmholz equation,

$$\left[\frac{\partial^2 X}{\partial x^2} + n^2(x)\frac{\Omega_j^2}{c^2} - k_z^2\right]X(x) = 0, \tag{2}$$

and appropriate boundary conditions. Here, $k_z = 5\pi \times 10^6$ m^{-1} is the z component of the total wave vector, Ω_j is the composite-cavity mode frequency, and $n(x)$ reflects the refractive index variation in the x direction. In particular, we assume

$$n(x) = \begin{cases} n_g = 3.6, & \text{in the passive gaps between lasers} \\ n_s = 3.61, & \text{in the active laser sections.} \end{cases}$$

The boundary conditions require that the electric field and its first derivative are continuous at each refractive index step and that they vanish at infinity. As in Ref. [26] we use sine functions in the active section and exponential functions in the passive section. Such solutions of the Helmholz Eq. (2) satisfy the orthogonality relation

$$\int_{-\infty}^{\infty} n^2(x) X_j(x) X_{j'}(x) dx = \delta_{jj'}\mathcal{N}, \tag{3}$$

where $\delta_{jj'}$ is the Kronecker delta and $\mathcal{N} = (n_b^2/2)(3w_0 + 2d_0)$ is a normalization constant with $n_b = 3.6$, $w_0 = 4$ μm, and $d_0 = 4$ μm.

The time evolutions of the complex-valued electric field amplitude $E_j(t)$ associated with the composite-cavity mode $X_j(x)$ and the carrier density $N_s(t)$ in laser stripe s are governed by

$$\frac{dE_j}{dt} = -i(\Omega_j - \nu_j)E_j - \gamma E_j + \gamma \sum_{j'} \left\{ \sum_s K_{jj'}^s [(1 + \beta N_s) - i\alpha\beta(1 + N_s)] \right\} E_{j'},$$

$$\frac{dN_s}{dt} = \Lambda - (N_s + 1) - \sum_{j,j'} K_{jj'}^s (1 + \beta N_s) \mathrm{Re}[E_j E_{j'}^*]. \tag{4}$$

Here the index $j = \{1, 2, 3\}$ refers to the three composite-cavity modes that are considered (Fig. 1), $s = \{A, B, C\}$ refers to the three lasers, and the star denotes complex conjugation; see Refs. [24,26] for details of the derivation. Most importantly, coupling between lasers occurs via the evanescent electric field in the lateral x direction and depends on the laser distance $d_{s's}$ (or the width of the passive gap between the lasers) and the laser-width mismatch in the x direction $\Delta_{s's} = w_{s'} - w_s$. Note that Eqs. (4) depend on the coupling parameters $d_{s's}$ and $\Delta_{s's}$ implicitly via composite-mode frequencies Ω_j and the mode overlap integrals

$$K_{jj'}^s = \frac{n_s}{\mathcal{N}} \int_s X_j(x) X_{j'}(x) dx$$

over the respective active region s. We use typical semiconductor laser parameters, namely, the confinement factor $\Gamma = 0.1$, the differential gain coefficient $\xi = 2.5 \times 10^{-20}$ m^{-2}, the carrier density at transparency $N_{ts} = 2.0 \times 10^{24}$ m^{-3}, the electric field decay rate $\gamma_E = 2.0 \times 10^{11}$ s^{-1}, and the carrier decay rate $\gamma_N = 1.0 \times 10^9$ s^{-1}. This gives the normalized decay rate $\gamma = 100$ and gain coefficient $\beta \approx 5.2$. Each laser is pumped at four times threshold, that is, $\Lambda = 4$.

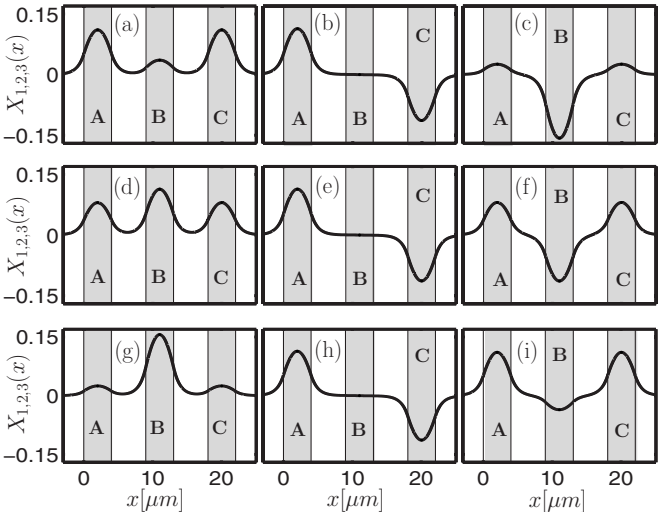

FIG. 1. The three considered lateral composite-cavity-mode profiles $X_1(x)$ to $X_3(x)$ for constant laser distance $d = 5.0$ μm, fixed lateral widths $w_A = w_C = 4.0$ μm of lasers A and B, and different lateral width of the middle laser, namely $\Delta_{BA} = -0.05$ μm in (a)–(c), $\Delta_{BA} = 0$ μm in (d)–(f), and $\Delta_{BA} = 0.05$ μm in (g)–(j).

Here, we define *locking* as a single-frequency solution of Eqs. (4),

$$E_j(t) = |E_j^0| e^{-i(\omega^0 t + \varphi_j^0)}, \quad N_s(t) = N_s^0, \tag{5}$$

where all nonzero complex-valued modal amplitudes have constant intensities $I_j = |E_j^0|^2$, the same optical frequency ω^0, a constant phase-shift φ_j^0, and each laser has a constant carrier density N_s^0. Simultaneous numerical continuation [27] of the composite-cavity mode profiles $X_j(x)$ and the locking solutions Eq. (5) unveils the stability diagram in the parameter plane of the laser distances and the width differences of the active laser sections.

III. IDENTICAL OUTER LASERS

Guided by the geometry of the system we first discuss the case where the two outer lasers are identical $w_A = w_C = 4.0$ μm and the distance between the middle laser and each outer laser is the same $d = d_{BA} = d_{CB}$. Such a setup is invariant under the interchange of the two outer lasers, which is mathematically a $\mathbb{Z}_2$ symmetry. Figure 1 shows the three composite-cavity mode profiles that arise in this symmetric configuration. *Symmetric* modes have identical electric field in the two outer lasers; see mode 1 in Figs. 1(a), 1(d), and 1(g) and mode 3 in Figs. 1(c), 1(f), and 1(i). *Antisymmetric* modes have an electric field of opposite sign in the two outer lasers; see mode 2 in Figs. 1(b), 1(e), and 1(h). The antisymmetric mode 2 is insensitive to changes of the width w_B. On the other hand, the symmetric modes do depend on w_B. Namely, mode 1 is dominant in the outer lasers if $\Delta_{BA} < 0$, and it is dominant in the middle laser if $\Delta_{BA} > 0$ [Figs. 1(a) and 1(g)]; the symmetric mode 3 exhibits the opposite behavior [Figs. 1(c) and 1(i)]; also compare with Ref. [17].

Figure 2 shows the complete bifurcation diagram of the stable locked solution [Eq. (5)]. The shaded regions of stable

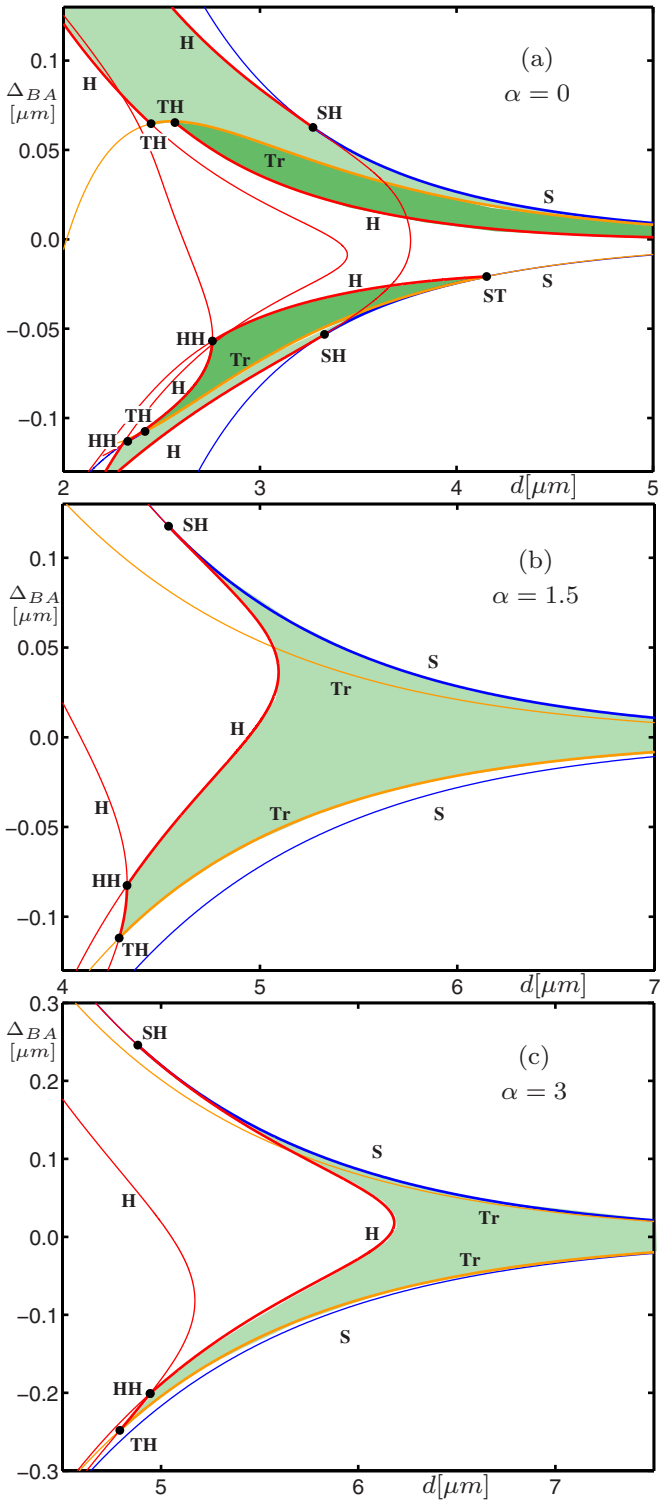

FIG. 2. (Color online) Stability diagram of locked solution (5) in the (d,Δ_{BA}) plane for the modal intensities $I_j=|E_j^0|^2$. Light shading indicates phase locking of two composite-cavity modes and dark shading indicates phase locking of three composite-cavity modes. The locking boundary is composed of curves of saddle-node (S), Hopf (H), and transcritical (Tr) bifurcations. The black dots indicate codimension-two saddle-node Hopf (SH), transcritical Hopf (TH), double Hopf (HH) bifurcations, and saddle-node transcritical (ST) bifurcations.

locking are bounded by saddle node (S), Hopf (H), and transcritical (Tr) bifurcation curves, which correspond to different locking-unlocking transitions. Light shading indicates that only the two symmetric composite-cavity modes contribute to locked solution (5), while in the dark shaded region all three modes contribute. Special bifurcation points (black dots) mark the switch over between different bifurcation curves or types of the locking boundary. A comparison between panels (a) and (b) of Fig. 2 shows a dramatic difference between the type and extent of stable locking regions for different values of α. This is illustrated further in Fig. 3, showing modal intensities $I_j=|E_j^0|^2$ of locked solutions (5) as well as the corresponding phase difference between the total electric field [Eq. (1)] in lasers A and B, ϕ_{AB}, and in lasers A and C, ϕ_{AC}, in dependence on Δ_{BA} for fixed d.

For $\alpha=0$ [Fig. 2(a)] we do not find stable locking near the central value of $\Delta_{BA}=0$, where the middle laser has the same frequency as the two outer lasers. Rather, locking occurs stably within two bands where the middle laser is sufficiently detuned (positively or negatively) from the two outer lasers. Furthermore, there are *four* different locking regions. The upper light shaded locking region in Fig. 2(a) is dominated by mode 3 with a relatively small contribution of mode 1 [Fig. 3, (a1)–(a3)]. The lower light shaded locking region is dominated by mode 1 with a relative small contribution of mode 3 [Fig. 3, (a1)–(a3)]. In both cases the intensity in the two outer lasers is identical. Furthermore, the phase difference ϕ_{AB} between the fields in lasers A and B is close to zero if $\Delta_{BA}<0$ and close to π if $\Delta_{BA}>0$ [Fig. 3, (a4)]. The phase difference ϕ_{AC} between lasers A and C is always zero [Fig. 3, (a5)]. In other words, the middle laser is in phase with the outer lasers ($\phi_{AB}\simeq 0$ and $\phi_{AC}\simeq 0$) if $\Delta_{BA}<0$ and out of phase with the outer lasers ($\phi_{AB}\simeq\pi$ and $\phi_{AC}\simeq 0$) if $\Delta_{BA}>0$. The transcritical bifurcation (Tr) indicates when mode 2 moves above its lasing threshold so that three composite-cavity modes are phase locked to a single frequency in the dark shaded region [Fig. 3, (a1)–(a3)]. Since mode 2 is antisymmetric, the total intensity in the two outer lasers now differs. Furthermore, for the three-mode locked state we find that $\phi_{AB}\neq 0$, π and $\phi_{AC}\neq 0$ [Fig. 3, (a4) and (a5)].

In contrast, for $\alpha=1.5$ (a typical value for quantum-well semiconductor lasers [23]), there is only a single stable locking region, which is located around the line $\Delta_{BA}=0$, where $w_B\sim w_{A,C}$ [Fig. 2(b)]. The locked solution is no longer dominated by a single composite-cavity mode, but is a coherent superposition of modes 1 and 3, which have comparable amplitudes [Fig. 3, (b1)–(b3)]. For the phase difference between lasers A and B we find that $\phi_{AB}\simeq\pi$ if $\Delta_{BA}=0$, meaning that the middle laser is out of phase with the outer lasers. Furthermore, ϕ_{AB} increases (decreases) slightly as Δ_{BA} increases (decreases). In particular, unlike in the case of $\alpha=0$, no stable locked solution is found where all three lasers oscillate in phase. The important difference is that for $\alpha>0$, the refractive index depends on the carrier density (index effect), which is what gives rise to the amplitude-phase coupling. As the middle laser typically equilibrates at a different carrier density compared to the two outer lasers, it can vary its *optical width*—defined as the product of the physical width and the refractive index. We find that for $\alpha=1.5$ stable locking occurs for a sufficiently large difference in the optical width

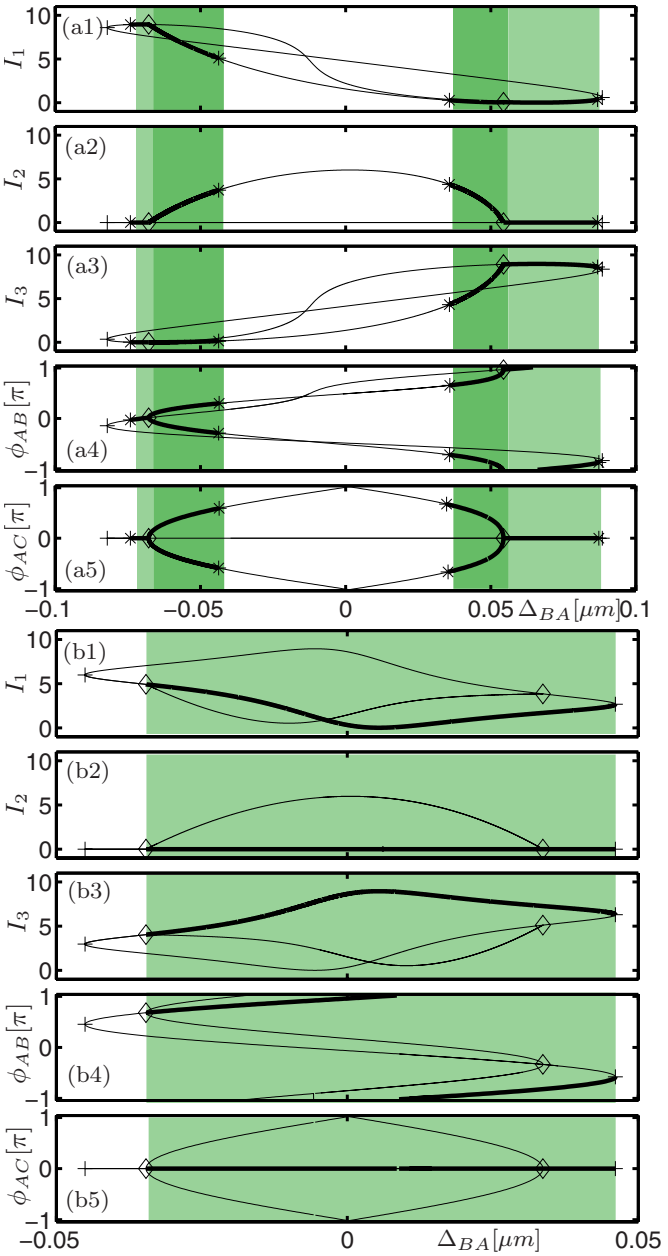

FIG. 3. (Color online) Modal intensities $I_j=|E_j^0|^2$ of locked solutions (5) [(a1)–(a3) and (b1)–(b3)], and the phase difference between the total electric field [Eq. (1)] in lasers A and B ϕ_{AB} [(a4) and (b4)] and in lasers A and C ϕ_{AC} [(a5) and (b5)]. Panels (a1)–(a5) are for $\alpha=0$ and $d=3$ μm and panels (b1)–(b5) are for $\alpha=1.5$ and $d=5.5$ μm. Stable solution branches (shading and thick curves) and unstable solution branches (thin curves) meet at saddle-node (+) and transcritical ($\diamond$) bifurcations, and they change stability at Hopf ($*$) bifurcations; compare with Fig. 2.

between the inner and the two outer lasers, even though the physical widths $w_{A,B,C}$ remain identical. This interesting effect due to amplitude-phase coupling can be interpreted as stable locking via "self-detuning" of the middle laser. As can be seen from Fig. 2(c) for $\alpha=3$, there are no qualitative changes in the locking region for higher values of α.

To summarize the effect of the linewidth-enhancement factor α, we show in Fig. 4 the different locking regions in

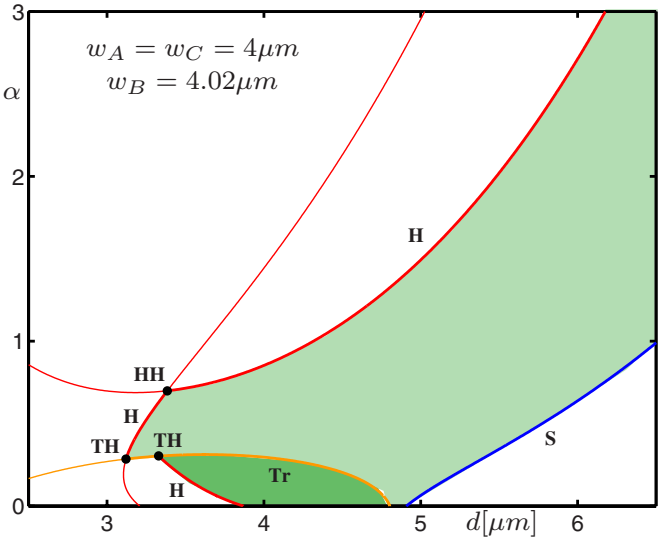

FIG. 4. (Color online) Stability diagram of locked solution (5) in the (d,α) plane for the modal intensities $I_j=|E_j^0|^2$ and $\alpha=1.5$. The locking boundary is composed of curves of saddle-node (S), Hopf (H), and transcritical (Tr) bifurcations. The black dots indicate codimension-two transcritical Hopf (TH) and double Hopf (HH) bifurcations. Labeling and color coding is as in Fig. 2.

the (d,α) plane for a small width difference $\Delta_{BA}=0.02$ μm. We find the characteristics of the locking regions from Fig. 2(a) to be typical for $\alpha<0.5$, whereas a locking region as in Figs. 2(b) and 2(c) is typical for $\alpha>0.5$. In Fig. 4, the transition between the two cases from Fig. 2 is marked by the transcritical bifurcation (Tr). Details of this transition in the (d,Δ_{BA}) plane involve several qualitative changes (codimension-three bifurcations) at intermediate values of α, which are beyond the scope of this paper. Finally, from Fig. 4 we can see that for $\alpha>0.5$ there is a single locking region bounded by a Hopf bifurcation on one side and a saddle-node bifurcation on the other side. As α increases this locking region shifts to larger d (weaker coupling) but it does not undergo any additional qualitative changes.

IV. BREAKING THE SYMMETRY

In Sec. III we discussed the $\mathbb{Z}_2$-symmetric situation with identical outer lasers. In Fig. 5 we present the effects of two different symmetry-breaking perturbations for $\alpha=1.5$. In Fig. 5(a) we introduce a small mismatch between the two outer lasers $\Delta_{CA}=w_C-w_A=0.02$ μm. As a result, the locking region shrinks in size and vanishes for $d>6.2$ μm. Furthermore, it is now bounded toward increasing d by a saddle-node bifurcation and toward decreasing d by a Hopf bifurcation. In addition we find a Hopf bifurcation curve at large d, which ends in codimension-two Bogdanov-Takens (BT) points. In Fig. 5(b) we keep the two neighboring lasers B and C identical $w_B=w_C=4$ μm and at a constant distance $d_{CB}=5$ μm, and explore the locking region in the (d_{AB},Δ_{BA}) plane. In this case, locking at large distance d_{BA} remains and is bounded by saddle-node bifurcations, but requires positive width difference Δ_{BC}. Toward decreasing d_{BA} the locking

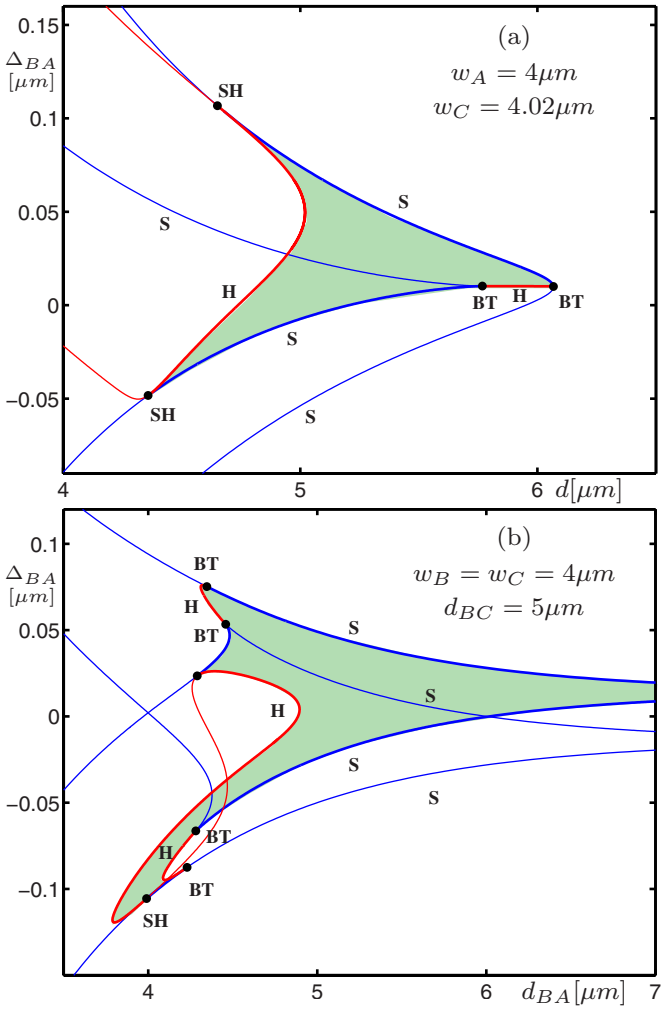

FIG. 5. (Color online) Stability diagram of locked solution (5) for the modal intensities $I_j=|E_j^0|^2$ and $\alpha=1.5$. Panel (a) shows the (d,Δ_{BA}) plane for $\Delta_{AC}=0.02$ μm, and panel (b) shows the (d_{BA},Δ_{BC}) plane for $w_A=w_B=4$ μm and $d_{BC}=5$ μm. Labeling and color coding is as in Fig. 2. Comparison with Fig. 2(b) reveals effects of nonidentical outer lasers and nonequal distances between the neighboring lasers.

region is bounded by saddle-node and Hopf bifurcations with several changes in the type of the locking boundary, which are indicated by codimension-two Bogdanov-Takens and saddle-node Hopf points.

As a consequence of the broken symmetry in the array, the stable locking region is modified: it changes its shape and shifts slightly toward positive Δ_{BA} in the (d,Δ_{BA}) plane, and the locking region may disappear for larger values of d. Furthermore, the transcritical locking boundaries from Fig. 2(b) unfold into saddle-node locking boundaries [28] in Fig. 5. Another difference from the symmetric case is that all three modes have nonzero intensity and contribute to locking as is shown in Fig. 6. Finally, none of the lasers are in phase: the phase difference between the total electric field (1) of laser A and B is in the range of $-\pi<\phi_{AB}<0$ and the phase difference between of laser A and C is in the range of $0<\phi_{AC}<\pi$.

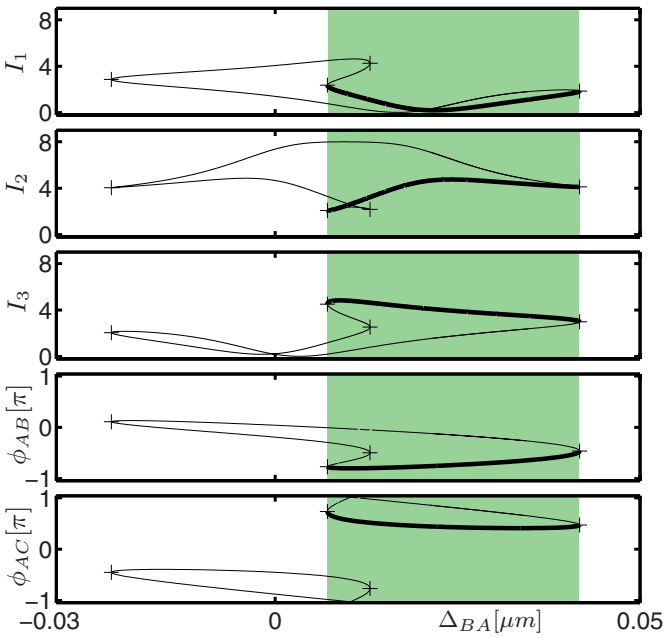

FIG. 6. (Color online) Modal intensities $I_j=|E_j^0|^2$ of locked solutions (5) and the phase difference between the total electric field [Eq. (1)] in lasers A and B ϕ_{AB} and in lasers A and C ϕ_{AC}; one parameter section of Fig. 5(a) for $d=5.5$ μm. Labeling and coloring is as in Fig. 3. Comparison with Fig. 3(b) reveals effects of nonidentical outer lasers on the behavior of individual composite-cavity modes.

V. CONCLUSION

We studied stable locking (single-frequency operation) of three laterally coupled laser oscillators by means of performing a bifurcation analysis of a mathematical model given as a field expansion in terms of three spatial composite-cavity modes. For the case where the outer lasers are identical we calculated the locking region in the plane of the distance between the lasers and the width difference of the middle laser. These two parameters specify the coupling between the lasers and the frequency detuning of the middle laser from the two outer lasers, respectively. We concentrated on the importance of the amplitude-phase coupling parameter α and showed that the locking characteristics is very different for low values of α, as opposed to larger values. Namely, for small amplitude-phase coupling ($\alpha\approx 0$), stable locking occurs for arbitrary coupling, but only within two sidebands where the middle laser has a different lateral width so that it is sufficiently detuned from the two outer lasers. Furthermore, we identified coupling conditions where the middle laser is in phase and out of phase with the outer lasers. For strong amplitude-phase coupling (such as for $\alpha=1.5$), on the other hand, locking occurs only for up to moderate/weak coupling and within a single band around where all three lasers have comparable lateral widths. Furthermore, we discussed modifications to locking that arise from perturbations to the symmetrical case of two identical outer lasers and equal distances between neighboring lasers. The effects uncovered here of amplitude-phase coupling and symmetry breaking in the array show that locked laser arrays would

require a careful manufacturing of lateral widths and distances with critical dependence on the type of the laser that is used. In particular, the lack of stable locking solution where all three lasers are in phase for $\alpha > 0.5$ may explain some of the great difficulties that are encountered in obtaining in-phase semiconductor laser arrays.

ACKNOWLEDGMENTS

This research was supported by Great Western Research Grant No. 18 under "Modeling and nonlinear dynamics of optical nanodevices: nanolasers and photonic nanocircuits."

[1] O. Hess and T. Kuhn, Phys. Rev. A **54**, 3347 (1996).
[2] E. Gehrig and O. Hess, Phys. Rev. A **57**, 2150 (1998).
[3] S. K. Mandre, I. Fischer, and W. Elsäßer, Opt. Commun. **244**, 355 (2005).
[4] *Diode Laser Arrays*, edited by D. Botez and D. Scifres (Cambridge University Press, Cambrdige, England, 1994).
[5] E. Kapon, J. Katz, and A. Yariv, Opt. Lett. **9**, 125 (1984).
[6] W. W. Chow, Opt. Lett. **10**, 442 (1985).
[7] W. W. Chow, J. Opt. Soc. Am. B **3**, 833 (1986).
[8] S. S. Wang and H. G. Winful, Appl. Phys. Lett. **52**, 1774 (1988).
[9] D. Mehuys and A. Yariv, Opt. Lett. **13**, 571 (1988).
[10] H. G. Winful and L. Rahman, Phys. Rev. Lett. **65**, 1575 (1990).
[11] P. Acedo, H. Lamela, B. Roycroft, G. Carpintero, and R. Santos, IEEE Photon. Technol. Lett. **14**, 1055 (2002).
[12] Y. Liu, H.-K. Liu, and Y. Braiman, Appl. Opt. **41**, 5036 (2002).
[13] J. J. Raftery, Jr., A. J. Danner, J. C. Lee, and K. D. Choquette, Appl. Phys. Lett. **86**, 201104 (2005).
[14] V. Raab and R. Menzel, Opt. Lett. **27**, 167 (2002).
[15] A. Jechow, V. Raab, R. Menzel, M. Cenkier, S. Stry, and J. Sacher, Opt. Commun. **277**, 161 (2007).
[16] B. Liu, Y. Liu, and Y. Braiman, Opt. Express **16**, 20935 (2008).
[17] W. W. Chow, J. Opt. Soc. Am. B **4**, 324 (1987).
[18] P. Ru, P. K. Jakobsen, J. V. Moloney, and R. A. Indik, J. Opt. Soc. Am. B **10**, 507 (1993).
[19] D. Merbach, O. Hess, H. Herzel, and E. Schöll, Phys. Rev. E **52**, 1571 (1995).
[20] R. Adler, Proc. IRE **34**, 351 (1946).
[21] Amplitude-phase coupling is a universal property of nonlinear oscillators and appears in various scientific disciplines under different names: in dynamical systems and biology one speaks of nonisochronicity or shear, in physics of nonlinear dispersion, and in engineering of self-phase modulation chirp.
[22] C. H. Henry, IEEE J. Quantum Electron. **18**, 259 (1982).
[23] W. Chow and S. Koch, *Semiconductor-Laser Fundamentals* (Springer-Verlag, Berlin, 1999).
[24] S. A. Shakir and W. W. Chow, Phys. Rev. A **32**, 983 (1985).
[25] W. Chow, IEEE J. Quantum Electron. **22**, 1174 (1986).
[26] H. Erzgräber, S. Wieczorek, and B. Krauskopf, Phys. Rev. E **78**, 066201 (2008).
[27] E. Doedel, A. Champneys, T. Fairgieve, Y. Kuznetsov, B. Oldeman, R. Paffenroth, B. Sandstede, X. Wang, and C. Zhang, Concordia University Technical Report, 2007 (available from http://indy.cs.concordia.ca/auto/).
[28] Y. Kuznetsov, *Elements of Applied Bifurcation Theory* (Springer, New York, 2004).